# GSK3a, not GSK3b, drives hippocampal NMDAR-dependent LTD via tau-mediated spine anchoring

**Article** *in* The EMBO Journal · November 2020

DOI: 10.15252/embj.2020105513



**7 authors**, including:

Jonathan E. Draffin
Spanish National Research Council
**9** PUBLICATIONS **183** CITATIONS
SEE PROFILE

Xavier Sánchez-Sáez
University of Alicante
**6** PUBLICATIONS **49** CITATIONS
SEE PROFILE

Article

SOURCE DATA | TRANSPARENT PROCESS

THE EMBO JOURNAL

# GSK3α, not GSK3β, drives hippocampal NMDAR-dependent LTD via tau-mediated spine anchoring

Jonathan E Draffin[1], Carla Sánchez-Castillo[1], Alba Fernández-Rodrigo[1], Xavier Sánchez-Sáez[1,†], Jesús Ávila[1], Florence F Wagner[2] & José A Esteban[1,*]

## Abstract

**Glycogen synthase kinase-3 (GSK3) is an important signalling protein in the brain and modulates different forms of synaptic plasticity. Neuronal functions of GSK3 are typically attributed to one of its two isoforms, GSK3β, simply because of its prevalent expression in the brain. Consequently, the importance of isoform-specific functions of GSK3 in synaptic plasticity has not been fully explored. We now directly address this question for NMDA receptor-dependent long-term depression (LTD) in the hippocampus. Here, we specifically target the GSK3 isoforms with shRNA knockdown in mouse hippocampus and with novel isoform-selective drugs to dissect their roles in LTD. Using electrophysiological and live imaging approaches, we find that GSK3α, but not GSK3β, is required for LTD. The specific engagement of GSK3α occurs via its transient anchoring in dendritic spines during LTD induction. We find that the major GSK3 substrate, the microtubule-binding protein tau, is required for this spine anchoring of GSK3α and mediates GSK3α-induced LTD. These results link GSK3α and tau in a common mechanism for synaptic depression and rule out a major role for GSK3β in this process.**

**Keywords** AMPA receptor; BRD-0705; BRD-3731; long-term depression; synaptic plasticity

**Subject Categories** Neuroscience; Signal Transduction

**DOI** 10.15252/embj.2020105513 | Received 4 May 2020 | Revised 8 October 2020 | Accepted 13 October 2020

**The EMBO Journal (2020) e105513**

## Introduction

Processes of synaptic plasticity are fundamental mechanisms by which neurons alter the strength of their connections in an activity-dependent manner. Long-lasting forms of synaptic plasticity, such as long-term potentiation (LTP) and long-term depression (LTD), are likely to be both necessary and sufficient for learning and memory (Bliss & Collingridge, 1993; Takeuchi *et al*, 2014). The serine/threonine kinase glycogen synthase kinase 3 (GSK3) is perhaps the most prolific kinase in the central nervous system (Linding *et al*, 2007; Sutherland, 2011). GSK3 is centrally involved in the regulation of multiple cellular functions (Grimes & Jope, 2001), and it has been linked to several prevalent diseases, such as Alzheimer's disease, particularly through its role as a tau kinase (Ishiguro *et al*, 1993; Hernandez *et al*, 2013). In the context of synaptic plasticity, GSK3 has been proposed to act as a molecular switch between LTP and LTD in the hippocampus (Peineau *et al*, 2007). Mechanistically, GSK3 in CA1 pyramidal cells undergoes inhibitory serine phosphorylation during the induction of LTP, which must occur for the expression of LTP (Hooper *et al*, 2007; Zhu *et al*, 2007; Peineau *et al*, 2007; Dewachter *et al*, 2009). Conversely, GSK3 must be active for NMDA receptor-dependent LTD to be induced (Peineau *et al*, 2007). At the level of plasticity, these mechanisms mean that LTP inhibits LTD (Peineau *et al*, 2007). Indirectly, GSK3 has been linked to LTD by studies showing the requirement for phosphorylation of its substrates at GSK3 sites. A peptide that interferes specifically with GSK3-mediated phosphorylation of KLC2, for example, blocked LTD (Du *et al*, 2010). Along analogous lines, neuronal overexpression of a phospho-null form of PSD-95 that is unable to be phosphorylated at its GSK3 site also blocked LTD (Nelson *et al*, 2013).

GSK3 exists as two paralogs, commonly referred to as isoforms: GSK3α and GSK3β (Woodgett, 1990). The catalytic (kinase) domains of GSK3α and GSK3β share 90% sequence identity, which has presented an obstacle to the development of selective pharmacological inhibitors. On the other hand, their C-terminal sequences show greater divergence, and GSK3α contains a ~60 amino acid glycine-rich region at its N-terminus that is absent in GSK3β (Kaidanovich-Beilin & Woodgett, 2011). The GSK3 isoforms share activity towards some substrates, including β-catenin (Doble *et al*, 2007) and glycogen synthase (MacAulay *et al*, 2007; Patel *et al*, 2008). Similarly, GSK3β has long been recognised as an effective tau kinase (Ishiguro *et al*, 1993; Sperber *et al*, 1995; Spittaels *et al*, 2000; Terwel *et al*, 2008), but GSK3α also phosphorylates tau *in vivo,* albeit less effectively (Maurin

1 Centro de Biología Molecular Severo Ochoa, CSIC-Universidad Autónoma de Madrid, Madrid, Spain
2 Stanley Center for Psychiatric Research, Broad Institute of Massachusetts Institute of Technology and Harvard University, Cambridge, MA, USA
*Corresponding author. Tel: +34 911964637; E-mail: jaesteban@cbm.csic.es
†Present address: Department of Physiology, Genetics and Microbiology, University of Alicante, Alicante, Spain

*et al*, 2013). Nevertheless, a number of other substrates display some degree of isoform specificity (Soutar *et al*, 2010).

Neuronal functions of GSK3, including those in synaptic plasticity, have typically been attributed to GSK3β, with few exceptions (Maurin *et al*, 2013). In fact, in most of the aforementioned studies on GSK3 in synaptic plasticity, the role of GSK3α was either not investigated, or the tools used were incapable of distinguishing between the two isoforms. This longstanding bias towards GSK3β is probably due to the prevalent expression of this isoform in the brain (Yao *et al*, 2002). However, both GSK3α and GSK3β are highly expressed in the nervous system (Woodgett, 1990), and mouse models deficient in GSK3α or GSK3β display different behavioural abnormalities (Kaidanovich-Beilin *et al*, 2009). In fact, recent studies have hinted at the importance of the α isoform in synaptic plasticity. For example, inhibition of GSK3α, but not GSK3β, was required for LTP (Shahab *et al*, 2014). GSK3α also controls structural plasticity of dendritic spines. Specifically, spine shrinkage induced by NMDA (cLTD) requires only GSK3α (Cymerman *et al*, 2015). Despite these advances, the isoform responsible for NMDA receptor-dependent functional LTD is still not known.

In this work, we specifically targeted the GSK3 isoforms with shRNA knock-down and novel isoform-selective drugs to dissect their roles in LTD. Using electrophysiological and live imaging approaches, we find that GSK3α, but not GSK3β, is required for LTD and is transiently anchored in dendritic spines during LTD induction. Interestingly, we also find that the microtubule-binding protein tau, which plays key roles in Alzheimer's disease, is required for this spine anchoring of GSK3α, and for GSK3α-induced LTD. Therefore, these results lead us to challenge the longstanding notion that GSK3β mediates LTD. Instead, we conclude that this role is played by GSK3α, via its activity-dependent spine recruitment through tau.

## Results

### shRNA knock-down of GSK3α, but not GSK3β, blocks NMDAR-dependent LTD

GSK3 activity is known to be required for NMDAR-dependent LTD (Peineau *et al*, 2007). However, the specific isoform requirements in this process are unknown. To test the requirement for the different GSK3 isoforms in LTD, we used an shRNA approach to specifically and independently ablate the activity of GSK3 isoforms. We took advantage of previously published shRNA designs for these experiments (Cymerman *et al*, 2015). We tested their effectiveness in our experimental setup by using a lentiviral vector to express the shRNAs in mouse primary hippocampal neurons and monitoring levels of GSK3α or GSK3β by Western blot (Fig EV1A). After 7–10 days of infection, shRNA against GSK3α produced a knock-down of GSK3α of 69 ± 8% (Fig EV1B) without effecting significant changes in GSK3β levels (82 ± 20%). Similarly, shRNA against GSK3β produced a knock-down of GSK3β of 57 ± 10% after 10–15 days of infection, without changing levels of GSK3α (95 ± 29%).

As a basis for evaluating isoform-specific roles of GSK3 in LTD, we first looked at the effect of GSK3 knock-down on basal synaptic transmission. To this end, we expressed shRNAs in CA1 of organotypic slice cultures prepared from rat hippocampus and performed paired whole-cell recordings of AMPA and NMDA receptor-mediated currents (Fig 1A). This experimental set-up allows us to examine the exclusive contribution of postsynaptic GSK3 towards the control of basal transmission. GSK3α shRNA had no significant effect on AMPA receptor-mediated EPSCs (93 ± 9% of uninfected currents; Fig 1B and C), while GSK3β knock-down produced a small but significant depression of transmission (80 ± 7% of uninfected EPSCs; Fig 1B and F). Neither GSK3α (136 ± 35% of uninfected) nor GSK3β (95 ± 23% of uninfected) shRNA significantly affected NMDA receptor-mediated EPSCs (Fig 1D and G, respectively). Accordingly, neither GSK3α nor GSK3β shRNAs produced a significant change in the ratio of AMPAR- to NMDAR-dependent synaptic responses (AMPA/NMDA; Fig 1E and H). In addition, these manipulations did not alter passive membrane properties of the neuron, such as input resistance, capacitance or holding current under voltage-clamp (Fig EV1C–H). Therefore, over the timescales tested, postsynaptic GSK3β knock-down leads to a modest depression of synaptic AMPA receptor-mediated currents, whereas GSK3α knock-down has no significant effect.

We then evaluated the contribution of GSK3α and GSK3β to LTD. NMDAR-dependent LTD is elicited under whole-cell patch-clamp recording with a low-frequency stimulation protocol (LFS, 300 pulses at 1 Hz to Schaffer collateral fibres) coupled to moderate depolarisation (–40 mV) of the postsynaptic CA1 cell. In our experimental set-up, this form of LTD was independent of metabotropic glutamate receptors (mGluRs), as similar synaptic depression was obtained in both control slices (to 46 ± 8% of baseline) and in slices pretreated with the non-selective group I/group II mGluR antagonist MCPG (to 42 ± 8% of baseline; Fig EV2). In addition, LTD induction by LFS has previously been shown to be blocked by the NMDA receptor antagonist APV (Mulkey & Malenka, 1992; Dudek & Bear, 1992). Therefore, this form of LTD depends on NMDA, but not mGlu receptors for its induction. To test the requirement for the different GSK3 isoforms in LTD, we expressed shRNAs against either GSK3α or GSK3β in CA1 of organotypic slice cultures prepared from rat hippocampus (Fig 2A). We then recorded from infected and uninfected CA1 pyramidal neurons while inducing NMDAR-dependent LTD in the slices. In slices injected with GSK3 shRNA viral vectors, a robust LTD was observed in uninfected cells (to 32 ± 5% of baseline; representative traces in Fig 2B, quantification in Fig 2C and D) and in neurons expressing shRNA against GSK3β (32 ± 7% of baseline). However, LTD was completely blocked in neurons expressing shRNA against GSK3α (99 ± 31% of baseline; Fig 2C and D). In this blockade, the whole population of endpoint values for depression was shifted, indicating a general reduction across recordings (Fig 2E). Thus, GSK3α, but not GSK3β, is required for NMDAR-dependent LTD.

### Pharmacological inhibition of GSK3α, but not GSK3β, blocks NMDAR-dependent LTD

Protein knock-down using shRNAs permits ablation of the activity of specific GSK3 isoforms to be confined to the postsynaptic cell. However, shRNA-mediated knock-down is intrinsically a chronic manipulation, since lentiviral-mediated expression of the corresponding shRNA is maintained for 7–15 days to ensure efficient protein knock-down. To employ a complementary approach and evaluate the relative contributions of GSK3 isoforms to synaptic function in an acute manner, we turned to recently developed

 

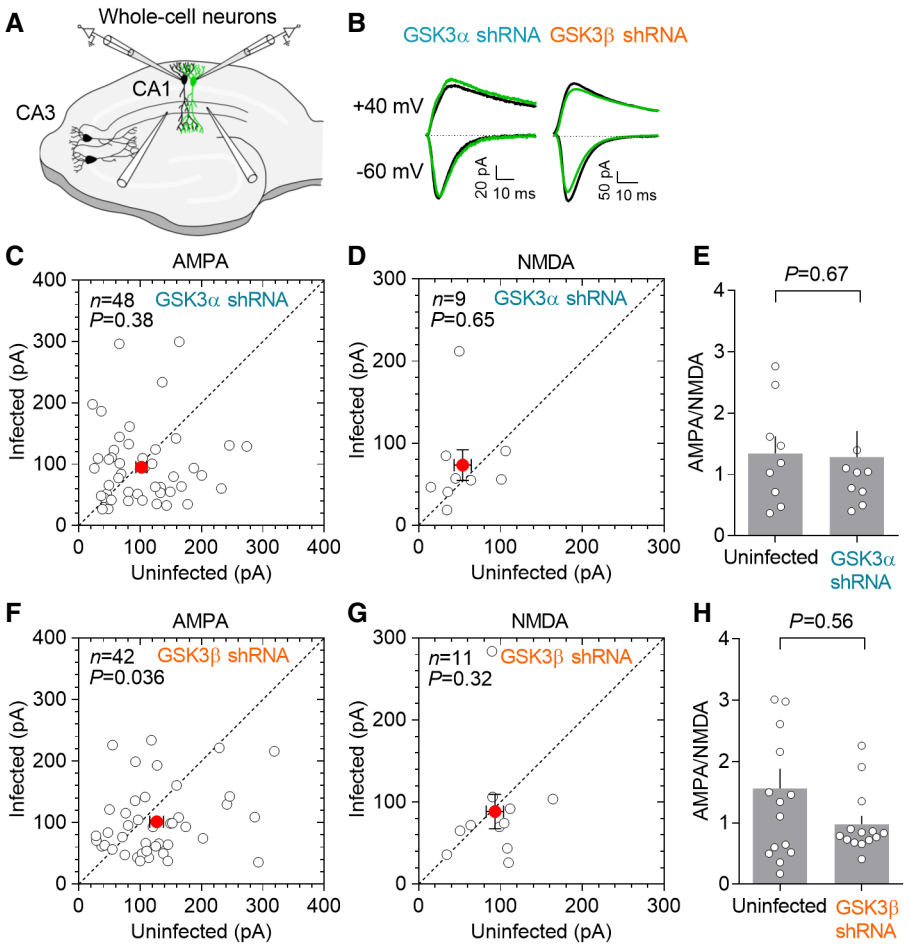


**Figure 1. Effect of GSK3 isoform knock-down on basal synaptic transmission.**

A Experimental scheme for (B–H). Whole-cell patch-clamp recordings were made from nearby pairs of uninfected and infected neurons in CA1 of organotypic hippocampal slices infected with lentivirus carrying shRNAs against GSK3α or GSK3β. EPSCs were elicited with CA3 Schaffer collateral stimulation.

B Representative traces for (C–H), showing evoked AMPAR- and NMDAR-mediated EPSCs (collected at −60 mV and +40 mV, respectively) in paired uninfected (black traces) and shRNA-expressing neurons (green traces).

C, D Scatter plots showing individual recordings of pairs of uninfected and infected neurons in slices expressing shRNA against GSK3α at −60 mV (AMPAR-mediated EPSCs; C) or at +40 mV (NMDAR-mediated EPSCs; D). Error bars represent SEM. Statistical significance was calculated according to the Wilcoxon signed-rank test.

E Quantification of individual (open circles) and average (grey bars) AMPA/NMDA ratios of neurons from uninfected and GSK3α shRNA lentivirus infected slices, where AMPAR-mediated current is taken as the peak response at −60 mV, and NMDAR-mediated current is measured at +40 mV at a latency of 60 ms following stimulation. Error bars represent SEM. Statistical significance was calculated according to the Mann–Whitney *U* test.

F, G As (C, D), for GSK3β. Error bars represent SEM. Statistical significance was calculated according to the Wilcoxon signed-rank test.

H As (E), for GSK3β. Error bars represent SEM. Statistical significance was calculated according to the Mann–Whitney *U* test.

Data information: Red circles represent the averages of all pairs in a given plot, and n denotes the number of cell pairs (panels C, D, F, G).

isoform-selective GSK3 inhibitors. Historically, inhibitors of GSK3 have not distinguished between the two isoforms because of high similarity between their respective catalytic domains, especially in the ATP-binding pocket. Recently, however, a single amino acid difference in these domains was exploited to design selective inhibitors of each GSK3 isoform (Wagner *et al*, 2018). These compounds, named BRD-0705 and BRD-3731, show 8–14 fold selectivity for GSK3α and GSK3β, respectively, in a cell-based BRET assay. As control, we employed an enantiomeric inactive compound, BRD-5648 (Wagner *et al*, 2018). For simplicity, these compounds will henceforth be referred to as inhibitors of GSK3α or GSK3β, or inactive control.

We first tested the effect of these inhibitors, along with the structurally similar but inactive control compound, on basal synaptic transmission. After incubating organotypic hippocampal slices for 1 h with selective inhibitors of GSK3α or GSK3β, or inactive control, we performed whole-cell recordings of AMPA and NMDA receptor-mediated EPSCs. Surprisingly, GSK3α inhibition dramatically decreased AMPA/NMDA ratios compared with inactive control ratios (mean of 1.05 ± 0.11 vs. 2.46 ± 0.18; Fig 3A and B), whereas GSK3β inhibition had no significant effect (mean of 2.60 ± 0.24). The population of AMPA/NMDA ratios is shifted uniformly with respect to inactive control ratios (Fig 3C), suggesting that inhibition of this isoform has a homogeneous effect throughout

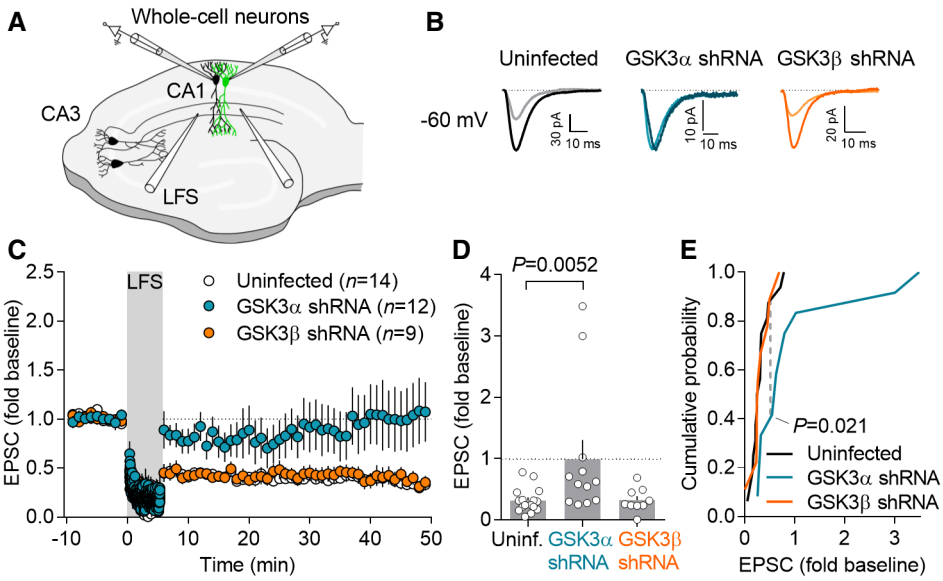


**Figure 2. shRNA knock-down of GSK3α, but not GSK3β, blocks NMDAR-dependent LTD.**

A Experimental scheme for (B–E). Whole-cell patch-clamp recordings were made from nearby pairs of uninfected and infected neurons in CA1 of organotypic hippocampal slices infected with lentivirus carrying shRNAs against GSK3α or GSK3β. EPSCs were elicited with CA3 Schaffer collateral stimulation, and low-frequency stimulation (LFS) was used to induce LTD.

B Representative traces for (C), where baseline responses (dark trace) are taken between 10 and 0 min before LTD induction, and responses after LTD induction (light trace) are taken between 40 and 45 min after the end of LTD induction.

C Time course of the peak AMPAR-mediated synaptic response to Schaffer collateral stimulation before, during, and after the induction of LTD by LFS (300 pulses at 1 Hz), in control (uninfected) and GSK3α (blue) or GSK3β (orange) shRNA-expressing neurons. Error bars represent SEM.

D Quantification of average synaptic depression from the last 5 min of the time course shown in (C). Error bars represent SEM. Statistical significance was calculated according to the Mann–Whitney *U* test.

E Cumulative frequency distribution of the ESPC values plotted in (D). Statistical significance was calculated according to the Kolmogorov–Smirnov test.

the synaptic responses we recorded. To confirm whether this effect was truly due to GSK3 inhibition, we carried out similar experiments with the general GSK3 inhibitors AR-A014418 (AR-18) and CHIR-99021 (CHIR). These two inhibitors do not distinguish between GSK3α and GSK3β isoforms, but they are highly specific for GSK3 versus closely related kinases, such as cdk2 or cdk5 (Bennett *et al*, 2002; Bhat *et al*, 2003). As shown in Fig 3D and E, these two inhibitors significantly decreased AMPA/NMDA ratios compared with their vehicle control (DMSO), and this effect was observed across the whole distribution of responses (Fig 3F). To note, it has been previously reported that another broad GSK3 inhibitor, SB415286, does not alter basal synaptic transmission (Peineau *et al*, 2007). However, this inhibitor may be less specific with respect to cyclin-dependent kinases (Chin *et al*, 2005).

Finally, as a complementary approach to assess the synaptic effects on GSK3 inhibition, we drove GSK3 phosphorylation at the inactivation sites (Ser21/9, for GSK3α and β, respectively) by pharmacological activation of Akt with the SC79. This is a small molecule activator that binds the PH domain of Akt and leads to its activation independently from phosphoinositide binding (Jo *et al*, 2012). As shown in Fig EV3, incubation with SC79 produced a strong increase in phosphorylation of Akt at the activating site (Thr308) and of GSK3 at the inhibitory sites (Ser9/21). These biochemical changes were accompanied by a significant decrease in AMPA/NMDA ratio, similar to the one observed by pharmacological inhibition of GSK3 (Fig 3D–F). This effect is consistent with a previous report of acute depression of synaptic transmission in hippocampal slices treated with SC79 (Pen *et al*, 2016). Therefore, all these results combined indicate that GSK3 activity (and particularly that of GSK3α) is required for the maintenance of synaptic transmission.

It is unclear why the GSK3α-selective inhibitor and the GSK3α shRNA produced different effects on basal synaptic transmission. It is possible that the effect of the inhibitor is only transient, and it disappears after the semi-chronic knock-down required for the shRNA experiments. Alternatively, it is also important to keep in mind that the inhibitor has access to the whole hippocampal slice, including presynaptic and postsynaptic compartments, as well as glial cells. In contrast, the shRNA knock-down is only expressed in the postsynaptic CA1 neuron. In any case, we decided to go forward and test these inhibitors on LTD, since we could always compare their effects with those of the isoform-specific shRNAs.

As described above, NMDAR-dependent LTD was induced in organotypic slices by LFS to Schaffer collaterals and monitored by whole-cell recording of CA1 pyramidal neurons (Fig 4A). In slices treated with the control compound, LTD could be reliably induced (35 ± 6% of baseline; Fig 4B–D) and no effect of the GSK3β inhibitor was observed compared to the inactive control (39 ± 10% of baseline). In contrast, LTD was blocked in slices

 

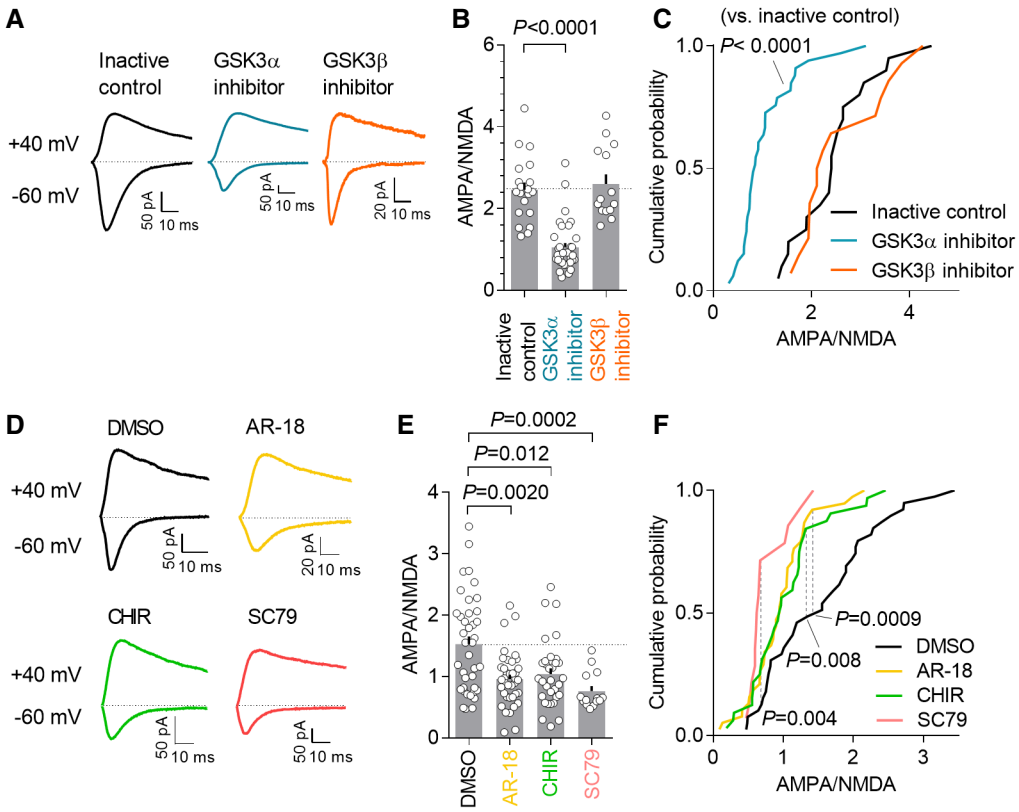


**Figure 3. Effect of acute pharmacological inhibition of GSK3 on basal synaptic transmission.**

A Representative traces for (B, C), showing evoked AMPAR- and NMDAR-mediated EPSCs (collected at −60 mV and +40 mV, respectively) in neurons from inactive control-, GSK3α or GSK3β inhibitor-treated slices (all at 10 μM). Slices were incubated with each compound for 1 h before recording, and during whole-cell recording itself. Compounds were also included in the internal solution of the recording pipette (all at 10 μM).

B Quantification of individual (open circles) and average (grey bars) AMPA/NMDA ratios of neurons from inactive control, GSK3α or GSK3β inhibitor-treated slices, where AMPAR-mediated current is taken as the peak response at −60 mV, and NMDAR-mediated current is measured at +40 mV at a latency of 60 ms following stimulation. Error bars represent SEM. Statistical significance was calculated according to the Mann–Whitney *U* test.

C Cumulative frequency distribution of the AMPA/NMDA ratios plotted in (B). Statistical significance was calculated using the Kolmogorov–Smirnov test.

D Representative traces for (E, F), showing evoked AMPAR- and NMDAR-mediated EPSCs (collected at −60 mV and +40 mV, respectively) in neurons from hippocampal slices treated with DMSO (vehicle control), AR-18 (10 μM), CHIR (1 μM) or SC79 (20 μM).

E, F As (B, C), for DMSO, AR-18, CHIR and SC79. Error bars represent SEM. Statistical significance was calculated according to the Mann–Whitney *U* test.

treated with GSK3α inhibitor (95 ± 7% of baseline; Fig 4B–D). As a control, LTD was also fully blocked in slices treated with the inhibitor AR-18, which does not distinguish between GSK3α and GSK3β (87 ± 6% of baseline; Fig 4B–D). Thus, an alternative, pharmacological approach to selectively reducing GSK3 isoform activity also reveals GSK3α, but not GSK3β, to be the isoform required for NMDAR-dependent LTD.

Given the decrease in AMPA/NMDA ratio produced by the GSK3α inhibitor (and AR-18), we also tested whether the failure to express LTD could be due to a flooring effect on synaptic transmission. To this end, we evaluated the effect of the GSK3α inhibitor on metabotropic glutamate receptor (mGluR)-dependent LTD, which relies on separate signalling cascades from those of NMDAR-dependent LTD, but also results in AMPAR synaptic removal (Snyder *et al*, 2001). As shown in Fig 4E–G, mGluR LTD was preserved in hippocampal slices treated with the GSK3α inhibitor and was comparable to slices treated with the inactive control. These results strengthen the interpretation that NMDAR-dependent LTD relies specifically on GSK3α. Incidentally, these data also indicate that GSK3α is not required for mGluR LTD (but see also McCamphill *et al*, 2020).

### Increased GSK3 activity induces synaptic depression

The previous experiments (described in Figs 2 and 4) demonstrate that activity of GSK3α, but not GSK3β, is necessary for the induction of NMDAR-dependent LTD. To test whether an increase in GSK3 activity is also sufficient to induce synaptic depression, we overexpressed recombinant EGFP-tagged versions of each isoform overnight in CA1 of organotypic slice cultures prepared from rat hippocampus. Both recombinant isoforms distributed throughout dendrites and dendritic spines (Fig EV4A) and were overexpressed with respect to the corresponding endogenous protein (EGFP-GSK3α; 220 ± 100% and EGFP-GSK3β: 150 ± 34% of endogenous; Fig EV4B and C). In addition, both recombinant proteins were less phosphorylated (relative to their total expression) than the

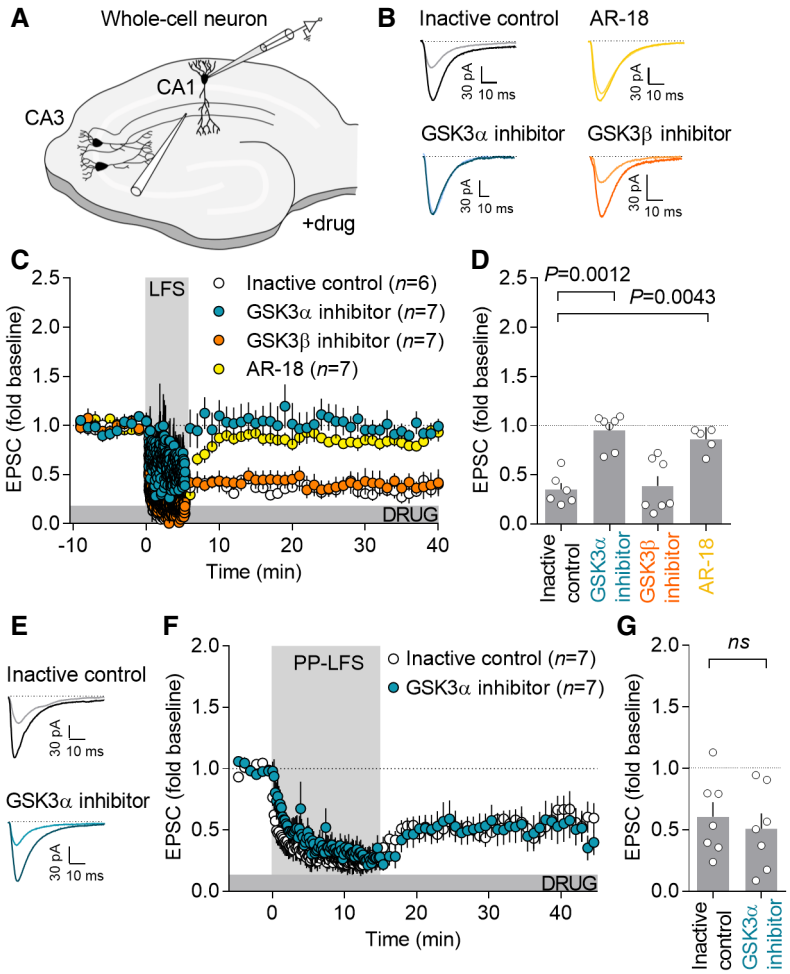


**Figure 4. Pharmacological inhibition of GSK3α, but not GSK3β, blocks NMDAR-dependent LTD.**

A Experimental scheme for (B–G). Whole-cell patch-clamp recordings were made from neurons in CA1 of organotypic hippocampal slices treated with inactive control, GSK3α or GSK3β inhibitor, or AR-18 (all at 10 μM). EPSCs were elicited with CA3 Schaffer collateral stimulation, and low-frequency stimulation (LFS) was used to induce LTD. For inactive control, GSK3α and GSK3β inhibitor compounds, the experiment was performed blind with respect to treatment group.

B Representative traces for (C, D), where baseline responses (dark trace) are taken between 10 and 0 min before LTD induction, and responses after LTD induction (light trace) are taken between 40 and 45 min after the end of LTD induction.

C Time course of the peak AMPAR-mediated synaptic response to Schaffer collateral stimulation before, during and after the induction of LTD by LFS (300 pulses at 1 Hz), in control (inactive control), GSK3α (blue) and GSK3β (orange) inhibitor, and AR-18-treated neurons (yellow). Drug treatment was for 1 h before recording at 10 μM for all compounds. Error bars represent SEM.

D Quantification of average synaptic depression from the last 5 min of the time course shown in (C). Error bars represent SEM and statistical significance was calculated according to the Mann–Whitney *U* test.

E As (B), for (F, G).

F Time course of the peak AMPAR-mediated synaptic response to Schaffer collateral stimulation before, during and after the induction of mGluR-dependent LTD by PP-LFS (900 paired pulses, separated by 50 ms, at 1 Hz), in control (inactive control) and GSK3α inhibitor-treated neurons (blue). Drug treatment was for 1 h before recording at 10 μM for all compounds. Representative traces for synaptic responses before (dark trace) and after (light trace) LTD induction are shown above the time course. Error bars represent SEM.

G Quantification of average synaptic depression from the last 5 min of the time course shown in (F). Error bars represent SEM. No statistically significant difference was found, according to the Mann–Whitney *U* test.

endogenous GSK3 isoforms (EGFP-GSK3α; 45 ± 34% and EGFP-GSK3β: 72 ± 17% of endogenous; Fig EV4B and D). Because of their higher expression and reduced phosphorylation, both overexpressed recombinant proteins are expected to increase net GSK3 activity in the infected cell.

To test whether an increase in the activity of either GSK3 isoform was able to induce LTD-like synaptic depression, we performed paired whole-cell patch-clamp recordings from infected and uninfected CA1 pyramidal neurons (Fig 5A). Indeed, evoked AMPAR-mediated currents were depressed by both EGFP-GSK3α (79 ± 13% of uninfected; Fig 5B and C) and EGFP-GSK3β (83 ± 11% of uninfected; Fig 5B and D) overexpression, while NMDAR-mediated currents were unaffected (EGFP-GSK3α: 105 ± 12% of uninfected, Fig 5B and E; EGFP-GSK3β: 110 ± 18% of uninfected; Fig 5B and

 

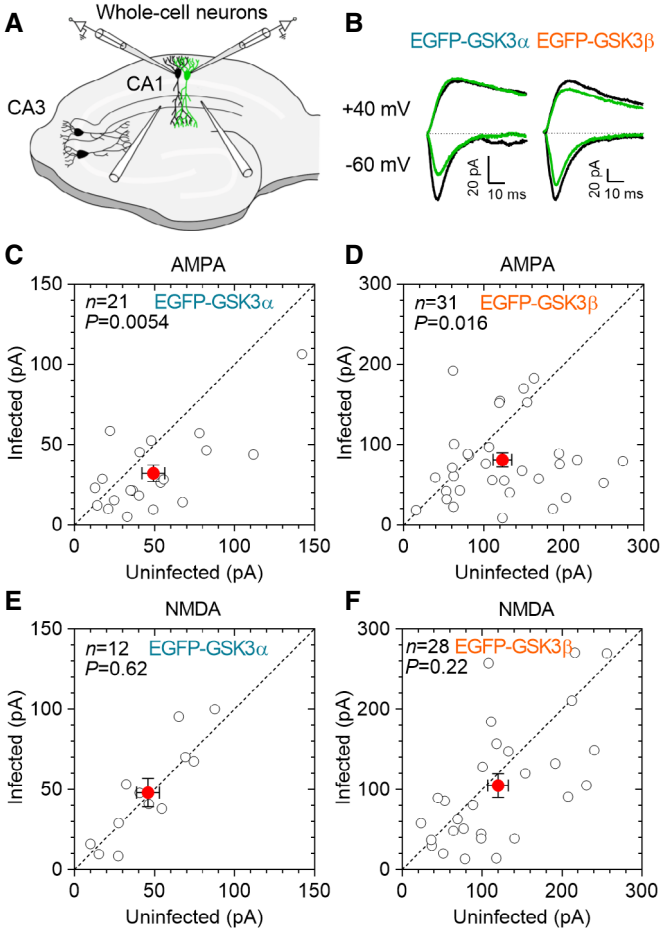


**Figure 5. Increased GSK3 activity induces synaptic depression.**

A Experimental scheme for (B–F). Whole-cell patch-clamp recordings were made from nearby pairs of uninfected and infected neurons in CA1 of organotypic hippocampal slices expressing EGFP-GSK3α or EGFP-GSK3β fusion proteins. EPSCs were elicited with CA3 Schaffer collateral stimulation.

B Representative traces for (C–F), showing evoked AMPAR- and NMDAR-mediated EPSCs (collected at −60 mV and +40 mV, respectively) in paired uninfected (black traces) and EGFP-GSK3α- or EGFP-GSK3β-expressing neurons (green traces).

C, D Scatter plots showing individual recordings of pairs of uninfected and infected neurons at −60 mV (AMPAR-mediated EPSCs) in slices expressing EGFP-GSK3α (C) or EGFP-GSK3β (D). Error bars represent SEM. Statistical significance was calculated according to the Wilcoxon signed-rank test.

E, F Scatter plots showing individual recordings of pairs of uninfected and infected neurons at +40 mV (NMDAR-mediated EPSCs) in slices expressing EGFP-GSK3α (E) or EGFP-GSK3β (F). Error bars represent SEM. Statistical significance was calculated according to the Wilcoxon signed-rank test.

Data information: Red circles represent the averages of all pairs in a given plot, and n denotes the number of cell pairs.

F). Thus, an increase in neuronal GSK3 activity, of either isoform, is sufficient to mimic LTD. Importantly, GSK3 overexpression did not alter passive membrane properties of the neuron, such as input resistance, membrane capacitance or holding current under voltage-clamp (Fig EV4E–J).

The fact that isoform specificity is lost with protein overexpression may be due to a saturation effect, as discussed below.

### GSK3α, but not GSK3β, is transiently anchored in dendritic spines during LTD

Since we saw a specific requirement for GSK3α in the expression of LTD, we sought to identify a cellular or molecular mechanism that explains this isoform specificity. Since this form of LTD has been shown to rely on the removal of AMPARs from the postsynaptic membrane (Beattie *et al*, 2000), we first looked at whether GSK3α and GSK3β were present in spines to different extents as compared to levels in adjacent dendrites. To this end, we co-expressed EGFP-GSK3α, EGFP-GSK3β or EGFP (as control), together with mCherry as a volume marker, in CA1 of rat organotypic hippocampal slices using biolistic methods (gene gun). As shown in Fig EV5A and B, spine/dendrite ratios were similar between EGFP-GSK3α, EGFP-GSK3β and EGFP, suggesting that there is no specific mechanism for spine recruitment of these proteins (at least for their recombinant form). In addition, spine volume, assessed from the spine/dendrite ratio of the mCherry volume marker, was also similar between neurons overexpressing EGFP-tagged GSK3 isoforms and plain EGFP (Fig EV5A and C). Therefore, even though GSK3 overexpression produced depression of AMPAR-mediated synaptic transmission (Fig 5B–D), this was not translated into changes in dendritic spine size.

To check whether there were isoform-specific differences at the level of protein dynamics with LTD, we used fluorescence recovery after photobleaching (FRAP). EGFP-tagged GSK3α or GSK3β was expressed in CA1 of rat organotypic hippocampal slices, in which "chemical" LTD (cLTD; 20 μM NMDA for 5 min) was then induced under live imaging conditions. Spines expressing EGFP-tagged GSK3 were photobleached, and the extent of fluorescence recovery was measured before (baseline), immediately after (cLTD), and 10 min subsequent to NMDAR activation (washout; Fig 6A and C). Approximately 85% of both the EGFP-GSK3α (Fig 6B and E) and EGFP-GSK3β (Fig 6D and E) fluorescence signal was recovered after 90 s post-bleaching, suggesting that over this period of time, only some 15% of GSK3, of either isoform, is stable in dendritic spines under basal conditions. In contrast, only 45% of EGFP-tagged GSK3α fluorescence was recovered immediately after cLTD induction, and this decrease in mobility disappeared after washout (85% recovery; Fig 6B and E). These results suggest that GSK3α is transiently anchored at spines during LTD induction. Strikingly, this anchoring was not observed for EGFP-GSK3β, which recovered to similar extents in baseline, cLTD and washout conditions (Fig 6D and E). Importantly, neither isoform changed its relative spine localisation as a result of cLTD (Fig 6F), and the extent of fluorescence recovery was independent of the initial accumulation of EGFP-GSK3 in the spine (Fig EV5D–G). Taken together, these observations suggest that GSK3α and GSK3β do not have intrinsic differences for their basal accumulation at spines, but GSK3α undergoes a specific anchoring/immobilisation within the spine in response to NMDA receptor activation during cLTD.

To check the effectiveness of our cLTD protocol, we tested biochemical markers typically associated with this form of synaptic depression. NMDA treatment *per se* was effective in inducing a classic marker of cLTD: GluA1 was dephosphorylated at its serine 845 site (Lee *et al*, 1998, 2000; He *et al*, 2011) following induction of cLTD

with NMDA (Fig 6G and H). Furthermore, cLTD induction produced robust dephosphorylation of both GSK3α and GSK3β at their inhibitory serine residues (Ser21/9, respectively; Fig 6G and H), as expected (Peineau *et al*, 2007). This effect had returned to baseline levels during washout of NMDA. This result suggests that both isoforms were transiently activated during cLTD induction. Nevertheless, only GSK3α, but not GSK3β, underwent transient anchoring in dendritic spines in response to NMDA treatment to induce cLTD.

### GSK3α spine anchoring requires the microtubule-associated protein tau

Although tau is most often thought of as an axonal protein, it is present in dendrites and spines and binds to microtubules in these compartments (Frandemiche *et al*, 2014). In fact, tau's function in dendritic spines has been proposed as a mechanism for beta-amyloid synaptic toxicity (Ittner *et al*, 2010). Given the capacity of tau to serve as a linker to structural scaffolding molecules, and its involvement in LTD (Kimura *et al*, 2014; Regan *et al*, 2015), we hypothesised that tau might serve as a binding target for GSK3α for its transient anchoring during LTD. Accordingly, we repeated the FRAP experiment in wild-type and tau knockout (de Barreda *et al*, 2010) mouse slices expressing EGFP-tagged GSK3α (see representative images in Fig 7A and C). Similar to the result in rat slices, approximately 85% of EGFP-tagged GSK3α was mobile under basal conditions in both wild-type and tau knockout slices (Fig 7B, D, and E). Following cLTD, however, GSK3α was anchored in wild-type (55%

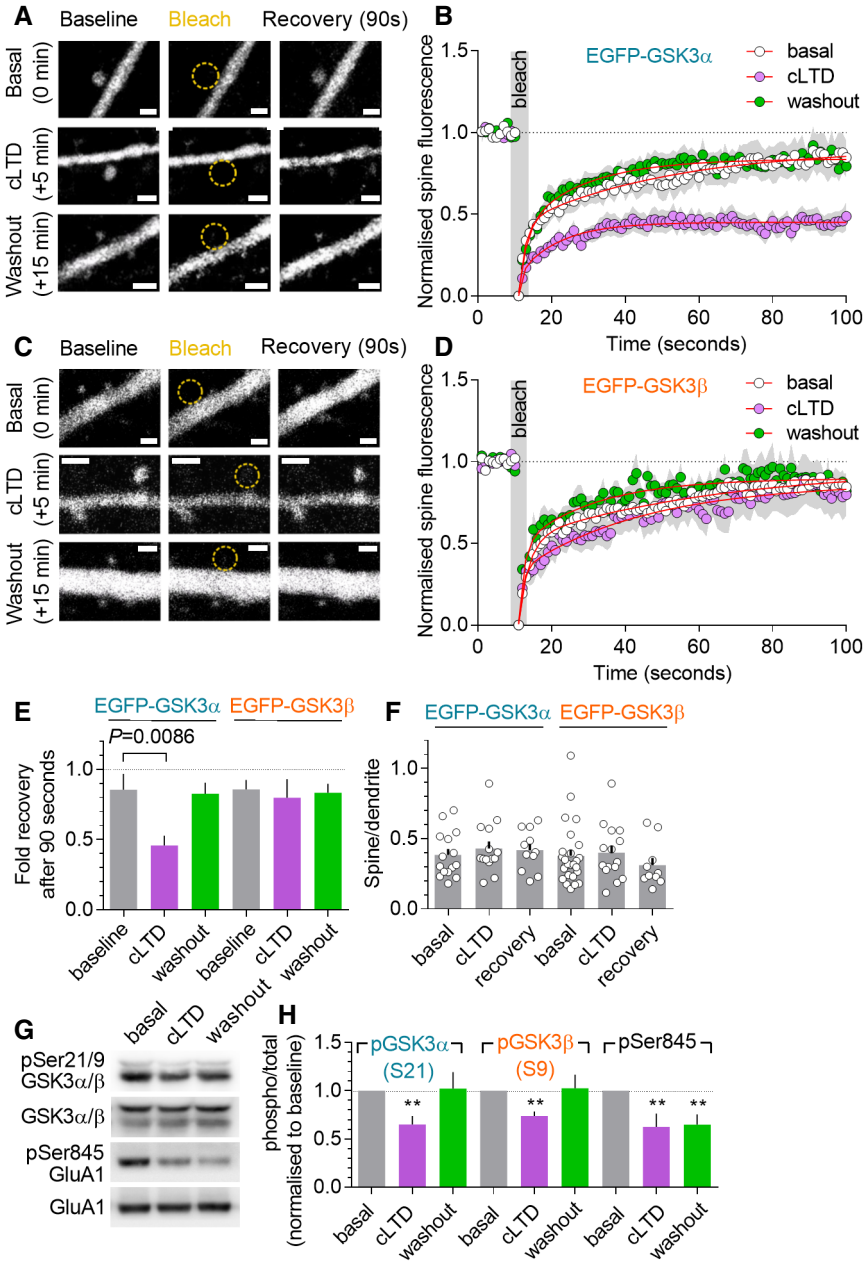


**Figure 6.**

**Figure 6. GSK3α, but not GSK3β, is transiently anchored in dendritic spines during LTD.**

A Representative confocal images from EGFP-GSK3α FRAP experiments. Upper left panel ("Baseline") shows EGFP-GSK3α expression in a dendrite and dendritic spine of organotypic slices cultured from rat hippocampus. The spine was bleached ("Bleach"; yellow dashed circle) and its fluorescence partially recovered 90 s later ("Recovery"). Single dendritic spines were imaged once per second for 10 s prior to, and for 90 s following, spine photobleaching. Such single FRAP experiments were performed on different spines during basal conditions ("basal"; upper panels), immediately after cLTD induction with 20 μM NMDA for 5 min ("cLTD"; middle panels), and immediately following 10 min of washout ("washout"; lower panels). Scale bars = 1 μm.

B Time course of fluorescence recovery during FRAP experiments described in A. White circles ("basal") show the average spine/dendrite fluorescence of FRAP on EGFP-GSK3α-expressing spines in slices prior to cLTD induction. Pink circles ("cLTD") show fluorescence in spines in which cLTD had been induced using 20 μM NMDA. Green circles ("washout") represent the average of spine fluorescence after NMDA washout for 10 min. Recovery trajectories for the three conditions are fitted with two-phase exponential curves (red lines).

C, D As (A, B) but for spines expressing EGFP-GSK3β. Scale bars = 1 μm.

E Quantification of last 10 s of fluorescence recovery (90–100 s) in (B, D). Bars represent mean ± SEM. Statistical significance was calculated according to the Mann–Whitney *U* test. $N = 12$, 11 and 11 spines for EGFP-GSK3α baseline, cLTD and washout groups and 20, 11 and 9 spines for EGFP-GSK3β baseline, cLTD and washout groups, respectively.

F Spine/dendrite ratios showing enrichment of EGFP-GSK3α or EGFP-GSK3β in "baseline", "cLTD" or "recovery" conditions. Bars represent mean ± SEM. Statistical significance was calculated according to the Mann–Whitney *U* test.

G Representative Western blots from whole extracts of organotypic slices incubated in ACSF (untreated; "baseline"), treated with 20 μM NMDA for 5 min ("cLTD") or treated with 20 μM NMDA for 5 min and allowed to recover in plain ACSF for 10 min ("washout"). Blots were probed for pSer21/9 GSK3α/β, total GSK3α/β, pSer845 GluA1 and total GluA1.

H Quantification of experiments as those shown in (G). Error bars represent SEM and statistical significance was calculated according to the Mann–Whitney *U* test. $N = 4$ independent experiments for all conditions. Asterisks (**) denote $P < 0.01$.

Source data are available online for this figure.

recovery after 90 s; Fig 7B and E) but not in tau knockout slices (86% recovery after 90 s; Fig 7D and E). Therefore, these results suggest that GSK3α requires tau for transient anchoring in the spine during LTD.

Crucially, EGFP-GSK3α was basally present in spines to similar extents in wild-type and tau knockout neurons as compared to levels in adjacent dendrite and showed no changes its relative spine localisation as a result of cLTD in either genetic context (Fig 7F). Therefore, blockade of GSK3α anchoring following cLTD in tau knockout neurons is not due to a difference in initial enrichment or a net alteration in trafficking between the spine and dendrite with cLTD. We therefore conclude that the presence of tau is required for the regulated anchoring of GSK3α during cLTD induction.

### Synaptic depression induced by GSK3α activity requires tau

Tau is a prominent player in Alzheimer's disease pathology, but also has a number of roles in synaptic function under physiological conditions (reviewed in Ittner & Ittner, 2018). Since phosphorylation of tau at the Ser396 GSK3 site is required for NMDAR-dependent LTD (Regan *et al*, 2015), and we had observed that LTD-induced GSK3α anchoring in the spine requires tau (Fig 7), we reasoned that the LTD-like synaptic depression induced by overexpression of GSK3α might be dependent on tau. To test this hypothesis, we prepared organotypic slices from tau knockout mice and overexpressed EGFP-tagged GSK3α in CA1 pyramidal neurons (Fig 8A). While GSK3α overexpression produced a similar synaptic depression in wild-type mouse slices (68 ± 11% of uninfected; representative traces in Fig 8B, quantification in Fig 8C) as in rat slices (Fig 5C), this depression was completely blocked in tau knockout slices (118 ± 14% of uninfected; Fig 8D). Importantly, given that the most prominent form of synaptic depression depends on the activation of NMDA receptors, the lack of effect of GSK3α overexpression on NMDA receptor function was preserved in tau knockout neurons (124 ± 25% of uninfected in wt [Fig 8E] versus 113 ± 16% of uninfected in tau knockout [Fig 8F]). Thus, the LTD-like synaptic depression induced by GSK3α overexpression requires the presence of tau, suggesting that tau is an intrinsic component of the mechanism by which GSK3α induces synaptic depression.

## Discussion

In this work, we have shown that the kinase GSK3α (but not GSK3β) and tau cooperate in choreographing the expression of NMDA receptor-dependent LTD. This conclusion is based on two main lines of evidence: (i) reduction of GSK3α (but not GSK3β) activity by novel pharmacological means or RNA interference blocks the expression of LTD and an increase in its activity induces LTD-like synaptic depression; and (ii) GSK3α (but not GSK3β) is transiently anchored in the spine in a tau-dependent manner during LTD. These lines of evidence indicate, respectively, that (i) postsynaptic GSK3α is necessary and sufficient for the expression of LTD; and (ii) that tau is a critical factor for stabilising GSK3α in spines and mediating its synaptic actions during LTD.

The notion of differential regulation and actions of GSK3α and GSK3β is becoming an emerging topic. This possibility arose with the different phenotypes of the GSK3α and GSK3β knockout mice (Hoeflich *et al*, 2000; MacAulay *et al*, 2007; Kaidanovich-Beilin & Woodgett, 2011). Both GSK3α knockout mice and heterozygous mice deficient in GSK3β display reduced exploratory activity and increased anxiety-associated behaviour (O'Brien *et al*, 2004; Bersudsky *et al*, 2008; Kaidanovich-Beilin *et al*, 2009). On the other hand, impaired sociability has only been reported for GSK3α knockout animals (Kaidanovich-Beilin *et al*, 2009), whereas memory deficits have been linked to GSK3β deficiency (Kimura *et al*, 2008). Impaired late-LTP and presynaptic function have also been reported for a neuron-specific GSK3α knockout (Maurin *et al*, 2013). In addition, it was recently reported that the pathophysiology of a mouse model of fragile X syndrome ($Fmr1^{-/y}$) can be corrected by specific

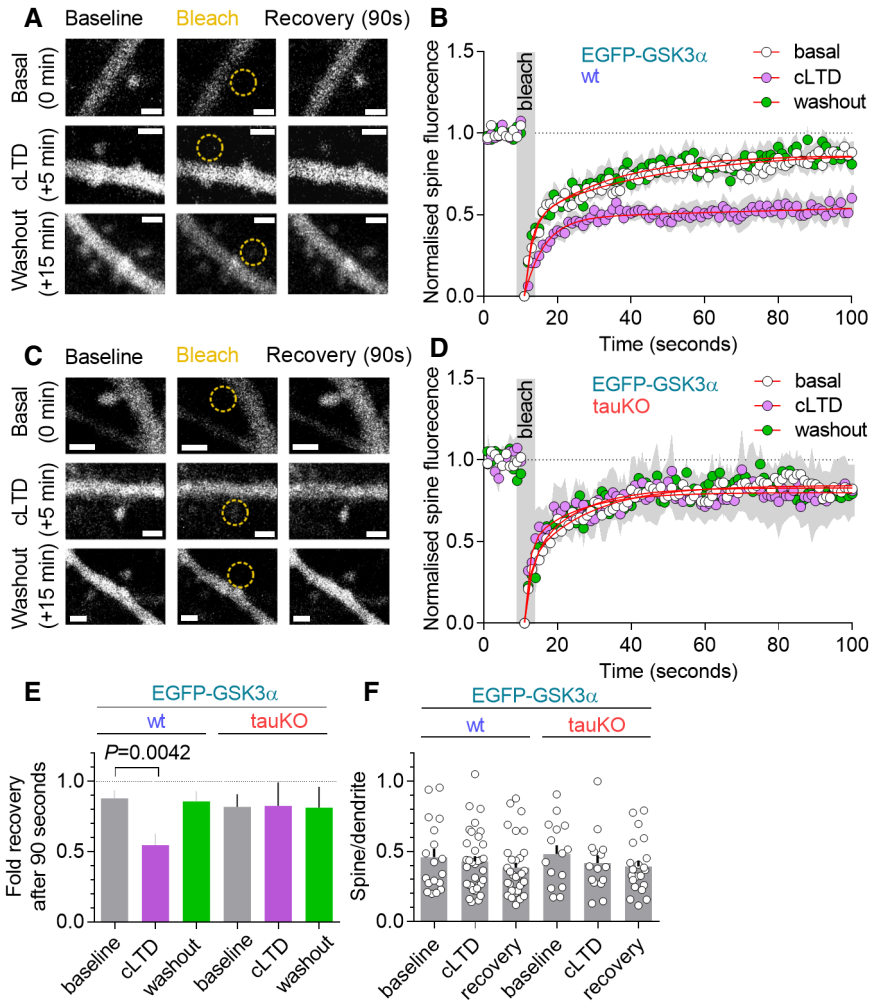


**Figure 7. GSK3α spine anchoring requires tau.**

A Representative confocal images from EGFP-GSK3α FRAP experiments in organotypic slices cultured from C57 wild-type mice. Upper left panel ("Baseline") shows EGFP-GSK3α expression in a dendrite and dendritic spine. The spine was bleached ("Bleach"; yellow dashed circle) and its fluorescence partially recovered 90 s later ("Recovery"). Single dendritic spines were imaged once per second for 10 s prior to, and for 90 s following, spine photobleaching. Such single FRAP experiments were performed on different spines during basal conditions ("basal"; upper panels), immediately after cLTD induction with 20 μM NMDA for 5 min ("cLTD"; middle panels), and immediately following 10 min of washout ("washout"; lower panels). Scale bars = 1 μm.

B Time course of fluorescence recovery during FRAP experiments described in (A). White circles ("basal") show the average spine/dendrite fluorescence of FRAP on EGFP-GSK3α-expressing spines in wild-type mouse slices prior to cLTD induction. Pink circles ("cLTD") show fluorescence in spines in which cLTD had been induced using 20 μM NMDA. Green circles ("washout") represent the average of spine fluorescence after NMDA washout for 10 min. Recovery trajectories for the three conditions are fitted with two-phase exponential curves (red lines).

C, D As (A, B) but in slices cultured from C57 tauKO mice. Scale bars = 1 μm.

E Quantification of last 10 s of fluorescence recovery (90–100 s) in (B, D). Error bars represent SEM and statistical significance was calculated according to the Mann–Whitney *U* test. *N* = 13, 11 and 12 spines for wt baseline, cLTD and recovery and 9, 7 and 5 spines for tauKO baseline, cLTD and recovery groups, respectively.

F Spine/dendrite ratios showing enrichment of EGFP-GSK3α in wild-type or tauKO slices in "baseline", "cLTD" or "recovery" conditions. Error bars represent SEM and statistical significance was calculated according to the Mann–Whitney *U* test.

inhibition of GSK3α (McCamphill *et al*, 2020). Incidentally, this study also showed that synaptic depression induced by mGluR activation was blocked by the GSK3α-selective inhibitor, in contrast with our results on mGluR LTD. We are not sure of the reason of this discrepancy, but it may be related to differences in the protocol for mGluR activation: application of the group I agonist DHPG ((S)-3,5-Dihydroxyphenylglycine; McCamphill *et al*, 2020) versus synaptic paired-pulse low-frequency stimulation (our study). In any case, these published results using animal models strongly suggest the direct participation of GSK3α and/or GSK3β in synaptic plasticity processes. Nevertheless, mechanistic explanations for differential functions at the level of neuronal physiology are, at best, scarce. This is also complicated by the fact that both GSK3α and GSK3β may play specific functions in neuronal development and proliferation of neuronal progenitors (Spittaels *et al*, 2002; Kim *et al*, 2006; Kim *et al*, 2009; Eom & Jope, 2009b). In the case of the neuronal

 

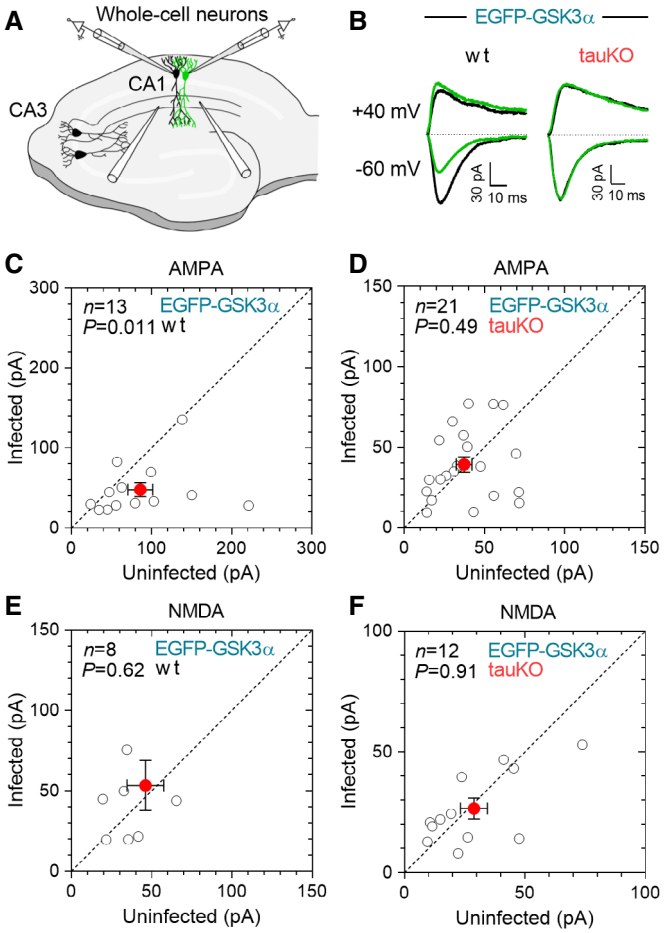


**Figure 8. Synaptic depression induced by GSK3α activity requires tau.**

A Experimental scheme for (B–F). Whole-cell patch-clamp recordings were made from nearby pairs of uninfected and infected neurons expressing EGFP-GSK3α in CA1 of organotypic hippocampal slices from C57 wt and tauKO mice. EPSCs were elicited with CA3 Schaffer collateral stimulation.

B Representative traces for (C–F), showing evoked AMPAR- and NMDAR-mediated EPSCs (collected at −60 mV and +40 mV, respectively) in paired uninfected (black traces) and EGFP-GSK3α-expressing neurons (green traces) in C57 wt or tauKO slices.

C–F Scatter plots showing individual recordings of pairs of uninfected and infected neurons at −60 mV (AMPAR-mediated EPSCs) in C57 wt (C) or tauKO slices (D), or at +40 mV (NMDAR-mediated EPSCs) in wt (E) or tauKO slices (F). Red circles represent the averages of all pairs in a given plot, and n denotes the number of cell pairs. In all cases, error bars represent SEM and statistical significance was calculated according to the Mann–Whitney *U* test.

GSK3α knockout, this is reflected in neuroanatomical changes in the hippocampus (Maurin *et al*, 2013).

In this study, using acute manipulations and differentiated neurons, we now show that GSK3 performs an isoform-specific function during NMDAR-LTD that relies on the anchoring of GSK3α (and not GSK3β) within dendritic spines. Subcellular targeting appears, therefore, as the main regulatory factor for the participation of GSK3 in this form of synaptic plasticity. Interestingly, the catalytic activity of both isoforms is presumably enhanced during LTD induction, as the phosphorylation of both isoforms is decreased after NMDAR activation. Nevertheless, only the activity of GSK3α becomes relevant for LTD expression. This interpretation strongly suggests that it is the subcellular colocalisation of GSK3α and its relevant substrate(s) that determines the functional outcome for synaptic strength. To note, this scenario is also compatible with our observation that overexpression of either GSK3α or GSK3β produces synaptic depression. Presumably, protein overexpression saturates the targeting mechanism, and both GSK3α and GSK3β will likely be competent to phosphorylate the relevant substrates. Interestingly, we observe that synaptic depression driven by GSK3 overexpression (in the absence of LTD induction) was not accompanied by a reduction in spine size. This result suggests that GSK3 activity is not sufficient to drive structural plasticity, even though GSK3α has been shown to be required for spine shrinkage during cLTD (Cymerman *et al*, 2015). To note, the dissociation between structural and functional aspects of synaptic depression has already been reported for other signalling molecules (Zhou *et al*, 2004; Thomazeau *et al*, 2020).

What are the potential substrates of GSK3 for synaptic depression? Several candidates have already been proposed. PSD-95 phosphorylation at threonine 19 by GSK3 leads to PSD-95 synaptic detachment and has been shown to be necessary for LTD expression (Nelson *et al*, 2013; this mechanism was shown for GSK3β but never tested for GSK3α). In addition, PICK1 (protein interacting with C kinase 1) is a synaptic protein that interacts with AMPARs and has also been shown to be phosphorylated by GSK3 (Yagishita *et al*, 2015; again, the effect was attributed to GSK3β, although isoform specificity was not tested). In this case, PICK1 phosphorylation enhances its interactions with AMPARs and therefore may fit with the proposed role of PICK1 in retaining internalised AMPARs during LTD (Daw *et al*, 2000; Kim *et al*, 2001).

Finally, a chief candidate for the specific actions of GSK3α in LTD is tau. We have shown that the anchoring of GSK3α in spines requires tau presence. GSK3α has been found to associate with tau in brain extracts (Sun *et al*, 2002), and this interaction may occur through 14-3-3 protein (Yuan *et al*, 2004). On the other hand, tau may be responsible for the delivery or spine localisation of the GSK3α binding partner, rather than acting as the partner *per se*. Conversely, since tau phosphorylation at Ser396 (a GSK3 site) is required for LTD (Regan *et al*, 2015), tau phosphorylation by GSK3α in the dendritic spine is a strong candidate to be the event required for LTD expression. Nevertheless, it is likely that the connections between GSK3 and tau for LTD are multiple and complex. For example, we are showing that synaptic depression induced by GSK3 overexpression does not occur in the absence of tau, arguing that tau is required downstream from GSK3 action, perhaps as a GSK3 substrate for LTD expression. On the other hand, tau is required for GSK3α anchoring in the spine in response to NMDAR activation. In this sense, tau may also be an upstream factor required for LTD induction (and consequently for GSK3 engagement). For example, we have recently described that CA1 pyramidal neurons lack extrasynaptic NMDAR currents in the tau knockout (Pallas-Bazarra *et al*, 2019). Extrasynaptic NMDARs have previously been linked to efficient LTD expression (Massey *et al*, 2004; Kollen *et al*, 2008; Papouin *et al*, 2012). Therefore, in this scenario, LTD may not be efficiently induced in the tau knockout because of the lack of extrasynaptic NMDARs, which in turn will fail to trigger GSK3's action in the spine. Therefore, we should be open to a multiplicity of mechanisms potentially linking tau, GSK3 and LTD.

Even though tau may participate in LTD at different levels, it is intriguing that its involvement with GSK3 is specific for GSK3α. Both GSK3α and GSK3β are capable of phosphorylating tau *in vivo* (Maurin *et al*, 2013). Nevertheless, cellular and molecular mechanisms may exist to implement specificity for GSK3α in binding to its target and in phosphorylating tau in the context of synaptic plasticity induction. That is, distinct regions of GSK3α, different from the equivalent regions of GSK3β, may serve as the locus for this anchoring specificity. Structural differences between the isoforms have been linked to functional differences in some cases. For example, GSK3β contains a nuclear localisation sequence that directs a subportion of it to the nucleus (Meares & Jope, 2007), whereas the N-terminal region of GSK3α results in its nuclear exclusion (where this latter effect may be overcome by calcium signalling; Azoulay-Alfaguter *et al*, 2011). However, in most cases in which a differential role for one isoform or the other has been identified, no structural basis is known. Neither GSK3 isoform contains a canonical binding domain, implying that the loci of covalent interactions are likely to vary according to the binding target. For example, studies of deletion and point mutants suggest the requirement of an N-terminal region (common to both isoforms) for binding of GSK3 to p53 (Eom & Jope, 2009a), but for sites on the C-terminal lobe for binding to GSK3 binding protein (GBP) and Axin (Ferkey & Kimelman, 2002). Although the N- and C-terminal domains are those that differ most between GSK3α and GSK3β and therefore would be good bets for harbouring the relevant difference for isoform-specific anchoring during LTD, the two isoforms nevertheless differ at 10% of sites in their large catalytic domains. Since single amino acid differences (many of them in the catalytic domain) have been shown to differentially (and dramatically) affect GSK3β binding to the Wnt signalling proteins Axin and Frat (Fraser *et al*, 2002), the possibility that isolated differences in the kinase domain might be responsible for conferring isoform specificity towards the binding target of GSK3α during LTD should not be overlooked.

Lastly, our results may also bear implications for the role of GSK3 in Alzheimer's disease. A mechanistic parallel has previously been noted between LTD and Alzheimer's disease pathology, particularly with respect to beta-amyloid synaptic toxicity (Hsieh *et al*, 2006; Shankar *et al*, 2008; Li *et al*, 2009; Alfonso *et al*, 2014; Knafo *et al*, 2016). Therefore, even if outside of the scope of this work, these new data suggest that the role of GSK3α in synaptic depression associated with Alzheimer's disease may have been overlooked.

## Materials and Methods

### Ethics statement

All procedures were approved by the bioethics committee of the Consejo Superior de Investigaciones Científicas (CSIC) and adhered to the guidelines set out in the European Community Council Directives (86/609/EEC).

### Primary hippocampal neuron culture

Primary hippocampal neurons for the biochemical evaluation of shRNA effectiveness were cultured from postnatal day 0–1 CD1 mice essentially as described previously (Beaudoin *et al*, 2012). Briefly, hippocampi were dissected from P0–P1 mice and the tissue disaggregated by trypsinisation. Cells were washed, counted and plated on poly-L-lysine-treated multi-well plates (Falcon) at a density of 25,000 cells/cm$^2$ in Neurobasal medium (Gibco) with B27 supplement (Invitrogen). Medium was changed at weekly intervals. Neurons were infected at 7 days *in vitro* for 7–15 days.

### Organotypic hippocampal slice cultures

Organotypic hippocampal slices were prepared from postnatal day 5–7 Wistar rats and CD1 mice essentially as described previously (Stoppini *et al*, 1991). Briefly, hippocampi were dissected from the brain in partially frozen dissection medium gassed with carbogen (5% $CO_2$/95% $O_2$) and 400 μm-thick slices prepared with a tissue chopper (Stoelting) in sterile conditions. Individual slices were placed on permeable membrane (Merck-Millipore) kept moist by slice culture medium. Slices were maintained at 35.5°C in a 5% $CO_2$ environment until use.

### Acute slice preparation

Acute whole-brain slices for biochemical and electrophysiological studies were prepared from 2- to 4-week-old Wistar rats using a Leica VT1200S vibratome (Leica). The rat was briefly anaesthetised using dry ice sublimated with water, and the brain removed and placed in partially frozen $Ca^{2+}$-free dissection medium saturated with 5% $CO_2$/95% $O_2$. After 1 min of cooling, the brain was placed on filter paper and a single cut made coronally so as to remove tissue rostral to the hippocampus. Another cut was made to remove the cerebellum, and the brain was glued (Loctite Super Glue-3) to the vibratome platform against a block of agarose (3% in water) such that the path of the blade would produce approximately coronal slices, dorsal to ventral, terminating at the agarose block. The cut at the base of the cerebellum and the angle of the base of the agarose block deviated from the coronal plane by approximately 10 degrees (Bischofberger *et al*, 2006). Such a slicing angle is more precisely orthogonal than the coronal plane to the direction of fibre alignment from CA3 to CA1 in the hippocampus and therefore improves synaptic responses and slice health. The mounted brain was covered with partially frozen $Ca^{2+}$-free dissection medium and the medium was gassed with 5% $CO_2$/95% $O_2$ during slicing. Slices were cut with a thickness of 300 μm, with a blade speed of 0.05–0.10 mm/s and a vibration amplitude of 0.60 mm. Freshly cut slices were placed in ACSF gassed with 5% $CO_2$/95% $O_2$, in a submersion-type chamber at 32°C. After 1 h, the incubator was brought to 25°C and the ACSF allowed to cool for 15 min, at which point the slices were considered ready for experimental manipulation.

### Primary antibodies

Antibodies used for western blotting were phospho GSK3α/β [Ser21/9] (Cell Signalling; #9331), GSK3α/β (Invitrogen; #44610), phospho-Akt [Thr308] (Cell Signalling; #9275), Akt (Cell Signalling; #9272), phospho-GluA1 [Ser845] (Thermo Fisher; OPA1-04118) and GluA1 (Millipore; #AB1504).

 

### Drugs

Pharmacological compounds used were as follows: AR-A014418 (AR-18; Sigma Aldrich); CHIR-99021 (CHIR; Tocris); SC79 (Tocris); BRD-5648, BRD-0705, BRD-3731, (inactive control, GSK3α inhibitor and GSK3β inhibitor, respectively; property of Broad Institute of MIT/Harvard, Mass. USA); RS-MCPG (MCPG; Tocris). Other compounds were purchased from Sigma and Merck-Millipore.

### DNA constructs

EGFP-tagged rat wild-type GSK3α and GSK3β constructs were generated by reverse transcription of total RNA extracted from rat forebrain, and PCR amplification of the resulting cDNA. Primers for PCR were as follows: GSK3α; 5'-CAGGACAGATCTATGAGCGGCGGC GGGCCTTC-3' (forward); 5'-CATCACGGTACCTCAGGAAGAGTTAG TGAGGGTAGGTGTGGC-3' (reverse); GSK3β: 5'-CAGGACAGATCTA TGTCGGGGCGACCGAGAACC-3' (forward); 5'-CATCACGGTACCTC AGGTAGAGTTGGAGGCTGATGC-3' (reverse). The resulting DNA was purified (PCR Clean-up kit; Macherey-Nagel) and digested with restriction enzymes (New England Biolabs) for ligation (Takara DNA Ligation Kit, Clontech) into pEGFP-C1 vector. All constructs were cloned into pSinRep5 for expression using Sindbis virus. For shRNA knock-down of mouse GSK3 isoforms, lentiviral vectors were developed according to the target sequences defined in the laboratory of Jacek Jaworski (Cymerman *et al*, 2015). pCI-mCherry was used for mCherry expression.

### Expression of recombinant proteins

For the expression of recombinant proteins and shRNAs in hippocampal CA1 pyramidal neurons in organotypic slice cultures, slices were prepared from postnatal day 5–7 rats and mice and cultured for 5–14 days, as described above. Sindbis virus- and biolistic-mediated expression of recombinant proteins was for 15–20 h, and lentiviral delivery of shRNAs for 7–15 days with infection the day after slice preparation. For lentivirus-mediated expression of shRNAs in primary hippocampal neurons, concentrated virus was added directly to the cell culture medium.

### Electrophysiology

Voltage-clamp whole-cell recordings were obtained from pyramidal cells in CA1 organotypic hippocampal slices, with the aid of transmitted light illumination. The recording chamber was perfused with ACSF containing 0.1 mM picrotoxin, 4 μM 2-chloroadenosine, and gassed with 5% $CO_2$/95% $O_2$. Patch recording pipettes (3–6 MΩ) were filled with internal solution (115 mM $CsMeSO_4$, 20 mM CaCl, 10 mM HEPES, 2.5 mM $MgCl_2$, 4 mM $Na_2$-ATP, 0.4 mM Na-GTP, 10 mM sodium phosphocreatine, 0.6 mM EGTA and 10 mM lidocaine n-ethyl bromide). Synaptic responses were evoked with bipolar electrodes using single-voltage pulses (200 μs, up to 20 V). Stimulating electrodes were placed among Schaffer collateral fibres approximately 300 μm from the recorded cells. A cut was made between CA3 and CA1 regions to isolate CA3 soma from back-propagated action potentials during Schaffer collateral stimulation. For paired recordings, infected and uninfected (control) cells within 50 μm of one another were identified using fluorescence illumination, and patched and recorded from simultaneously. Such a configuration ensures that (i) manipulations induced by viral infection occur exclusively in the postsynaptic cell, since only CA1 (and not CA3) cells are infected, and that (ii) gross regional variations in slice connectivity are controlled for, since patched cells are at a similar distance from stimulated afferent (Schaffer collateral) fibres. Synaptic AMPAR-mediated responses are measured as the peak of responses at −60 mV, and NMDA receptor (NMDAR)-mediated responses at +40 mV, at a latency when AMPAR responses have fully decayed (105 ms). For the recording of AMPA/NMDA ratios, average responses are first collected at −60 mV, then at +40 mV, after any post-transition increase in holding current has stabilised, and finally at 0 mV, to control for clamp quality. For paired recordings and AMPA/NMDA ratios, synaptic responses were averaged over 50–100 trials. NMDAR-dependent LTD was induced by pairing low-frequency Schaffer collateral stimulation (300 pulses at 1 Hz) with mild depolarisation of the postsynaptic cell (to −40 mV). mGluR-dependent LTD was induced by low-frequency Schaffer collateral stimulation with 900 paired pulses separated by 50 ms and delivered at 1 Hz. Time courses before and after LTD induction were collected at 0.2 Hz. Response measurements were averaged such that 12 trials contributed to each graphed data point. All electrophysiological recordings were carried out with Multiclamp 700A/B amplifiers (Axon Instruments) in conjunction with pCLAMP9/10 software.

### Live confocal fluorescence imaging

Confocal fluorescence images were acquired with a Zeiss LSM710 microscope with 63X NA 1.2 water C-Apochromat objective and a 488 nm laser, in conjunction with Zeiss Zen2010B SP1 software. Imaging of organotypic slices was performed in a chamber continuously perfused with ACSF gassed with carbogen (5% $CO_2$/95% $O_2$) at 29°C. For FRAP experiments with cLTD induction, spine-dendrite pairs were identified and EGFP signal in the spine was photobleached with high laser intensity for 5 s. Recovery of fluorescence following photobleaching was measured at 1-s intervals for 90 s. Multiple spines in the same field of view were bleached and imaged in some cases, provided they belonged to dendrites projecting from different cells. For each experimental condition (baseline, cLTD and recovery), FRAP was performed on a different spine. Image analysis was carried out with ImageJ 1.51p software. For each time point in an individual FRAP experiment, the following operations were performed: (i) spine/dendrite ratios of EGFP signal were calculated by drawing circular ROIs around spine heads and adjacent dendritic shafts; (ii) spine/dendrite ratios of integrated density were generated therefrom. Since spine/dendrite ratios are collected in local pairs, this method controls for local variation in overexpression intensity; (iii) residual fluorescence at the point of maximum photobleaching was subtracted; (iv) background was subtracted, and (v) all points were normalised to the baseline average.

### Western blotting

Whole-cell extracts were prepared from organotypic or acute hippocampal slices and primary neuronal cultures by homogenising with a yellow-tipped pipette in 100 μl RIPA buffer (50 mM Tris–HCl pH 7.4, 150 mM NaCl, 1% Triton X-100, 0.5% sodium deoxycholate, 0.1% SDS) per mg of tissue or 5 $cm^2$ of cultured cells and incubating

on ice for 15 min. Cell debris was removed by centrifugation at 14,000 × *g* for 10 min at 4°C. Extracts were quantified using a bicinchoninic acid (BCA)-based kit (Thermo Fisher; standard microplate procedure) in combination with a FLUOStar OPTIMA plate reader (BMG Labtech; 560 nm absorption), and analysed by SDS–PAGE and Western blotting, with the primary antibodies described above. Labelled membranes were incubated with undiluted enhanced chemiluminescent HRP substrate (Millipore) for 5 min and photographed using an ImageQuant LAS 4000 Mini biomolecular imager (GE Healthcare). Signal intensities were quantified under linear conditions using ImageJ 1.51p (public domain software developed at the US National Institutes of Health) after background subtraction.

#### Statistical analysis

Statistical significance was calculated with a Mann–Whitney *U* test for unpaired data, unless stated otherwise; with ANOVA when comparing multiple groups; with a Wilcoxon signed-rank test for normalised paired data; and with a Kolmogorov–Smirnov test to compare cumulative distributions.

## Data availability

This study includes no data deposited in external repositories.

**Expanded View** for this article is available online.

### Acknowledgements
We would like to thank Jacek Jaworski for his generous provision of shRNA plasmids for GSK3 isoform knock-down, Noemí Pallas-Bazarra for arranging our use of the tau knockout animals. We also thank the members of the Esteban laboratory for their critical reading of the manuscript, and the personnel at the fluorescence microscopy facility of the CBMSO (SMOC) for their expert technical assistance. This work was supported by grants from the Spanish Ministry of Science (SAF2017-86983-R) to JAE. JED, CS-C and AF-R were recipients of pre-doctoral contracts from the Spanish Ministry of Science.

### Author contributions
JED carried out most of the experimental work. CS-C carried out mGluR LTD experiments and AF-R carried out confocal imaging and quantification of EGFP-GSK3/mCherry in dendritic spines. XS-S assisted in the generation of GSK3 and shRNA expression vectors. JA and FFW provided unique reagents and assisted in writing the manuscript. JED and JAE designed research and wrote the manuscript.

### Conflict of interest
FFW previously consulted for a biotechnology company on a GSK3-related project and is an inventor on multiple GSK3-related patent applications filed by the Broad Institute.

## References

Alfonso S, Kessels HW, Banos CC, Chan TR, Lin ET, Kumaravel G, Scannevin RH, Rhodes KJ, Huganir R, Guckian KM *et al* (2014) Synapto-depressive effects of amyloid beta require PICK1. *Eur J Neurosci* 39: 1225 – 1233

Azoulay-Alfaguter I, Yaffe Y, Licht-Murava A, Urbanska M, Jaworski J, Pietrokovski S, Hirschberg K, Eldar-Finkelman H (2011) Distinct molecular regulation of glycogen synthase kinase-3α isozyme controlled by Its N-terminal region. *J Biol Chem* 286: 13470 – 13480

de Barreda EG, Pérez M, Ramos PG, de Cristobal J, Martín-Maestro P, Morán A, Dawson HN, Vitek MP, Lucas JJ, Hernández F *et al* (2010) Tau-knockout mice show reduced GSK3-induced hippocampal degeneration and learning deficits. *Neurobiol Dis* 37: 622 – 629

Beattie EC, Carroll RC, Yu X, Morishita W, Yasuda H, Von Zastrow M, Malenka RC (2000) Regulation of AMPA receptor endocytosis by a signaling mechanism shared with LTD. *Nat Neurosci* 3: 1291 – 1300

Beaudoin GMJ, Lee S-H, Singh D, Yuan Y, Ng Y-G, Reichardt LF, Arikkath J (2012) Culturing pyramidal neurons from the early postnatal mouse hippocampus and cortex. *Nat Protoc* 7: 1741 – 1754

Bennett CN, Ross SE, Longo KA, Bajnok L, Hemati N, Johnson KW, Harrison SD, MacDougald OA (2002) Regulation of Wnt signaling during adipogenesis. *J Biol Chem* 277: 30998 – 31004

Bersudsky Y, Shaldubina A, Kozlovsky N, Woodgett JR, Agam G, Belmaker RH (2008) Glycogen synthase kinase-3β heterozygote knockout mice as a model of findings in postmortem schizophrenia brain or as a model of behaviors mimicking lithium action: Negative results. *Behav Pharmacol* 19: 217 – 224

Bhat R, Xue Y, Berg S, Hellberg S, Ormö M, Nilsson Y, Radesäter AC, Jerning E, Markgren PO, Borgegård T *et al* (2003) Structural insights and biological effects of glycogen synthase kinase 3-specific inhibitor AR-A014418. *J Biol Chem* 278: 45937 – 45945

Bischofberger J, Engel D, Li L, Geiger JRP, Jonas P (2006) Patch-clamp recording from mossy fiber terminals in hippocampal slices. *Nat Protoc* 1: 2075 – 2081

Bliss TVP, Collingridge GL (1993) A synaptic model of memory: Long-term potentiation in the hippocampus. *Nature* 361: 31 – 39

Chin PC, Majdzadeh N, D'Mello SR (2005) Inhibition of GSK3β is a common event in neuroprotection by different survival factors. *Mol Brain Res* 137: 193 – 201

Cymerman IA, Gozdz A, Urbanska M, Milek J, Dziembowska M, Jaworski J (2015) Structural plasticity of dendritic spines requires GSK3α and GSK3β. *PLoS One* 10: e0134018

Daw MI, Chittajallu R, Bortolotto ZA, Dev KK, Duprat F, Henley JM, Collingridge GL, Isaac JTR (2000) PDZ proteins interacting with C-terminal GluR2/3 are involved in a PKC-dependent regulation of AMPA receptors at hippocampal synapses. *Neuron* 28: 873 – 886

Dewachter I, Ris L, Jaworski T, Seymour CMM, Kremer A, Borghgraef P, De Vijver H, Godaux E, Van Leuven F (2009) GSK3beta, a centre-staged kinase in neuropsychiatric disorders, modulates long term memory by inhibitory phosphorylation at serine-9. *Neurobiol Dis* 35: 193 – 200

Doble BW, Patel S, Wood GA, Kockeritz LK, Woodgett JR (2007) Functional redundancy of GSK-3α and GSK-3β in Wnt/β-catenin signaling shown by using an allelic series of embryonic stem cell lines. *Dev Cell* 12: 957 – 971

Du J, Wei Y, Liu L, Wang YT, Khairova R, Blumenthal R, Tragon T, Hunsberger JG, Machado-Vieira R, Drevets W *et al* (2010) A kinesin signaling complex mediates the ability of GSK-3beta to affect mood-associated behaviors. *Proc Natl Acad Sci USA* 107: 11573 – 11578

Dudek SM, Bear MF (1992) Homosynaptic long-term depression in area CA1 of hippocampus and effects of N-methyl-D-aspartate receptor blockade. *Proc Natl Acad Sci USA* 89: 4363 – 4367

Eom T-Y, Jope RS (2009a) GSK3 beta N-terminus binding to p53 promotes its acetylation. *Mol Cancer* 8: 14

 

Eom TY, Jope RS (2009b) Blocked inhibitory serine-phosphorylation of glycogen synthase kinase-3α/β impairs in vivo neural precursor cell proliferation. *Biol Psychiatry* 66: 494 – 502

Ferkey DM, Kimelman D (2002) Glycogen synthase kinase-3β mutagenesis identifies a common binding domain for GBP and Axin. *J Biol Chem* 277: 16147 – 16152

Frandemiche ML, De Seranno S, Rush T, Borel E, Elie A, Arnal I, Lante F, Buisson A (2014) Activity-dependent tau protein translocation to excitatory synapse is disrupted by exposure to amyloid-beta oligomers. *J Neurosci* 34: 6084 – 6097

Fraser E, Young N, Dajani R, Franca-Koh J, Ryves J, Williams RSB, Yeo M, Webster M-T, Richardson C, Smalley MJ *et al* (2002) Identification of the axin and frat binding region of glycogen synthase kinase-3. *J Biol Chem* 277: 2176 – 2185

Grimes CA, Jope RS (2001) The multifaceted roles of glycogen synthase kinase 3β in cellular signaling. *Prog Neurobiol* 65: 391 – 426

He K, Lee A, Song L, Kanold PO, Lee H-K (2011) AMPA receptor subunit GluR1 (GluA1) serine-845 site is involved in synaptic depression but not in spine shrinkage associated with chemical long-term depression. *J Neurophysiol* 105: 1897 – 1907

Hernandez F, Lucas JJ, Avila J (2013) GSK3 and tau: two convergence points in Alzheimer's disease. *J Alzheimers Dis* 33: S141 – S144

Hoeflich KP, Luo J, Rubie EA, Tsao MS, Jin O, Woodgett JR (2000) Requirement for glycogen synthase kinase-3β in cell survival and NF-κB activation. *Nature* 406: 86 – 90

Hooper C, Markevich V, Plattner F, Killick R, Schofield E, Engel T, Hernandez F, Anderton B, Rosenblum K, Bliss T *et al* (2007) Glycogen synthase kinase-3 inhibition is integral to long-term potentiation. *Eur J Neurosci* 25: 81 – 86

Hsieh H, Boehm J, Sato C, Iwatsubo T, Tomita T, Sisodia S, Malinow R (2006) AMPAR removal underlies Aβ-induced synaptic depression and dendritic spine loss. *Neuron* 52: 831 – 843

Ishiguro K, Shiratsuchi A, Sato S, Omori A, Arioka M, Kobayashi S, Uchida T, Imahori K (1993) Glycogen synthase kinase 3β is identical to tau protein kinase I generating several epitopes of paired helical filaments. *FEBS Lett.* 325: 167 – 172

Ittner LM, Ke YD, Delerue F, Bi M, Gladbach A, van Eersel J, Wölfing H, Chieng BC, Christie MJ, Napier IA *et al* (2010) Dendritic function of tau mediates amyloid-β toxicity in Alzheimer's disease mouse models. *Cell* 142: 387 – 397

Ittner A, Ittner LM (2018) Dendritic tau in Alzheimer's disease. *Neuron* 99: 13 – 27

Jo H, Mondal S, Tan D, Nagata E, Takizawa S, Sharma AK, Hou Q, Shanmugasundaram K, Prasad A, Tung JK *et al* (2012) Small molecule-induced cytosolic activation of protein kinase Akt rescues ischemia-elicited neuronal death. *Proc Natl Acad Sci USA* 109: 10581 – 10586

Kaidanovich-Beilin O, Lipina TV, Takao K, Van Eede M, Hattori S, Laliberté C, Khan M, Okamoto K, Chambers JW, Fletcher PJ *et al* (2009) Abnormalities in brain structure and behavior in GSK-3alpha mutant mice. *Mol. Brain* 2: 35

Kaidanovich-Beilin O, Woodgett JR (2011) GSK-3: functional insights from cell biology and animal models. *Front Mol Neurosci* 4: 40

Kim CH, Chung HJ, Lee HK, Huganir RL (2001) Interaction of the AMPA receptor subunit GluR2/3 with PDZ domains regulates hippocampal long-term depression. *Proc Natl Acad Sci USA* 98: 11725 – 11730

Kim WY, Zhou FQ, Zhou J, Yokota Y, Wang YM, Yoshimura T, Kaibuchi K, Woodgett JRR, Anton ES, Snider WDD (2006) Essential roles for GSK-3s and GSK-3-primed substrates in neurotrophin-induced and hippocampal axon growth. *Neuron* 52: 981 – 996

Kim WY, Wang X, Wu Y, Doble BW, Patel S, Woodgett JR, Snider WD (2009) GSK-3 is a master regulator of neural progenitor homeostasis. *Nat Neurosci* 12: 1390 – 1397

Kimura T, Yamashita S, Nakao S, Park JM, Murayama M, Mizoroki T, Yoshiike Y, Sahara N, Takashima A (2008) GSK-3β is required for memory reconsolidation in adult brain. *PLoS One* 3: e3540

Kimura T, Whitcomb DJ, Jo J, Regan P, Piers T, Heo S, Brown C, Hashikawa T, Murayama M, Seok H *et al* (2014) Microtubule-associated protein tau is essential for long-term depression in the hippocampus. *Philos Trans R Soc Lond B Biol Sci* 369: 20130144

Knafo S, Sánchez-Puelles C, Palomer E, Delgado I, Draffin JE, Mingo J, Wahle T, Kaleka K, Mou L, Pereda-Perez I *et al* (2016) PTEN recruitment controls synaptic and cognitive function in Alzheimer's models. *Nat Neurosci* 19: 443 – 453

Kollen M, Dutar P, Jouvenceau A (2008) The magnitude of hippocampal long term depression depends on the synaptic location of activated NR2-containing N-methyl-d-aspartate receptors. *Neuroscience* 154: 1308 – 1317

Lee HK, Kameyama K, Huganir RL, Bear MF (1998) NMDA induces long-term synaptic depression and dephosphorylation of the GluR1 subunit of AMPA receptors in hippocampus. *Neuron* 21: 1151 – 1162

Lee H-K, Barbarosie M, Kameyama K, Bear MF, Huganir RL (2000) Regulation of distinct AMPA receptor phosphorylation sites during bidirectional synaptic plasticity. *Nature* 405: 955 – 959

Li S, Hong S, Shepardson NE, Walsh DM, Shankar GM, Selkoe D (2009) Soluble oligomers of amyloid β protein facilitate hippocampal long-term depression by disrupting neuronal glutamate uptake. *Neuron* 62: 788 – 801

Linding R, Jensen LJ, Ostheimer GJ, van Vugt MATM, Jørgensen C, Miron IM, Diella F, Colwill K, Taylor L, Elder K *et al* (2007) Systematic discovery of in vivo phosphorylation networks. *Cell* 129: 1415 – 1426

MacAulay K, Doble BW, Patel S, Hansotia T, Sinclair EM, Drucker DJ, Nagy A, Woodgett JR (2007) Glycogen synthase kinase 3α-specific regulation of murine hepatic glycogen metabolism. *Cell Metab* 6: 329 – 337

Massey PV, Johnson BE, Moult PR, Auberson YP, Brown MW, Molnar E, Collingridge GL, Bashir ZI (2004) Differential roles of NR2A and NR2B-containing NMDA receptors in cortical long-term potentiation and long-term depression. *J Neurosci* 24: 7821 – 7828

Maurin H, Lechat B, Dewachter I, Ris L, Louis JV, Borghgraef P, Devijver H, Jaworski T, Van Leuven F (2013) Neurological characterization of mice deficient in GSK3α highlight pleiotropic physiological functions in cognition and pathological activity as Tau kinase. *Mol Brain* 6: 27

McCamphill PK, Stoppel LJ, Senter RK, Lewis MC, Heynen AJ, Stoppel DC, Sridhar V, Collins KA, Shi X, Pan JQ *et al* (2020) Selective inhibition of glycogen synthase kinase 3α corrects pathophysiology in a mouse model of fragile X syndrome. *Sci Transl Med* 12: eaam8572

Meares GP, Jope RS (2007) Resolution of the nuclear localization mechanism of glycogen synthase kinase-3: functional effects in apoptosis. *J Biol Chem* 282: 16989 – 17001

Mulkey RM, Malenka RC (1992) Mechanisms underlying induction of homosynaptic long-term depression in area CA1 of the hippocampus. *Neuron* 9: 967 – 975

Nelson CD, Kim MJ, Hsin H, Chen Y, Sheng M (2013) Phosphorylation of threonine-19 of PSD-95 by GSK-3β is required for PSD-95 mobilization and long-term depression. *J Neurosci* 33: 12122 – 12135

O'Brien WT, Harper ADA, Jové F, Woodgett JR, Maretto S, Piccolo S, Klein PS (2004) Glycogen synthase kinase-3β haploinsufficiency mimics the behavioral and molecular effects of lithium. *J Neurosci* 24: 6791 – 6798

Pallas-Bazarra N, Draffin J, Cuadros R, Antonio Esteban J, Avila J (2019) Tau is required for the function of extrasynaptic NMDA receptors. *Sci Rep* 9: 9116

Papouin T, Ladépêche L, Ruel J, Sacchi S, Labasque M, Hanini M, Groc L, Pollegioni L, Mothet JP, Oliet SHR (2012) Synaptic and extrasynaptic NMDA receptors are gated by different endogenous coagonists. *Cell* 150: 633 – 646

Patel S, Doble BW, MacAulay K, Sinclair EM, Drucker DJ, Woodgett JR (2008) Tissue-specific role of glycogen synthase kinase 3 in glucose homeostasis and insulin action. *Mol Cell Biol* 28: 6314 – 6328

Peineau S, Taghibiglou C, Bradley C, Wong TP, Liu L, Lu J, Lo E, Wu D, Saule E, Bouschet T *et al* (2007) LTP inhibits LTD in the hippocampus via regulation of GSK3beta. *Neuron* 53: 703 – 717

Pen Y, Borovok N, Reichenstein M, Sheinin A, Michaelevski I (2016) Membrane-tethered AKT kinase regulates basal synaptic transmission and early phase LTP expression by modulation of post-synaptic AMPA receptor level. *Hippocampus* 26: 1149 – 1167

Regan P, Piers T, Yi J-H, Kim D-H, Huh S, Park SJ, Ryu JH, Whitcomb DJ, Cho K (2015) Tau phosphorylation at serine 396 residue is required for hippocampal LTD. *J Neurosci* 35: 4804 – 4812

Shahab L, Plattner F, Irvine EE, Cummings DM, Edwards FA (2014) Dynamic range of GSK3α not GSK3β is essential for bidirectional synaptic plasticity at hippocampal CA3-CA1 synapses. *Hippocampus* 24: 1413 – 1416

Shankar GM, Li S, Mehta TH, Garcia-Munoz A, Shepardson NE, Smith I, Brett FM, Farrell MA, Rowan MJ, Lemere CA *et al* (2008) Amyloid-β protein dimers isolated directly from Alzheimer's brains impair synaptic plasticity and memory. *Nat Med* 14: 837 – 842

Snyder EM, Philpot BD, Huber KM, Dong X, Fallon JR, Bear MF (2001) Internalization of ionotropic glutamate receptors in response to mGluR activation. *Nat Neurosci* 4: 1079 – 1085

Soutar MPM, Kim W-Y, Williamson R, Peggie M, Hastie CJ, McLauchlan H, Snider WD, Gordon-Weeks PR, Sutherland C (2010) Evidence that glycogen synthase kinase-3 isoforms have distinct substrate preference in the brain. *J Neurochem* 115: 974 – 983

Sperber BR, Leight S, Goedert M, Lee VM (1995) Glycogen synthase kinase-3 beta phosphorylates tau protein at multiple sites in intact cells. *Neurosci Lett* 197: 149 – 153

Spittaels K, Van den Haute C, Van Dorpe J, Geerts H, Mercken M, Bruynseels K, Lasrado R, Vandezande K, Laenen I, Boon T *et al* (2000) Glycogen synthase kinase-3β phosphorylates protein tau and rescues the axonopathy in the central nervous system of human four-repeat tau transgenic mice. *J Biol Chem* 275: 41340 – 41349

Spittaels K, Van den Haute C, Van Dorpe J, Terwel D, Vandezande K, Lasrado R, Bruynseels K, Irizarry M, Verhoye M, Van Lint J *et al* (2002) Neonatal neuronal overexpression of glycogen synthase kinase-3β reduces brain size in transgenic mice. *Neuroscience* 113: 797 – 808

Stoppini L, Buchs PA, Muller D (1991) A simple method for organotypic cultures of nervous tissue. *J Neurosci Methods* 37: 173 – 182

Sun W, Qureshi HY, Cafferty PW, Sobue K, Agarwal-Mawal A, Neufield KD, Paudel HK (2002) Glycogen synthase kinase-3beta is complexed with tau protein in brain microtubules. *J Biol Chem* 277: 11933 – 11940

Sutherland C (2011) What are the *bona fide* GSK3 substrates? *Int J Alzheimers Dis* 2011: 1 – 23

Takeuchi T, Duszkiewicz AJ, Morris RGM (2014) The synaptic plasticity and memory hypothesis: encoding, storage and persistence. *Philos Trans R Soc Lond B Biol Sci* 369: 20130288

Terwel D, Muyllaert D, Dewachter I, Borghgraef P, Croes S, Devijver H, Van Leuven F (2008) Amyloid activates GSK-3β to aggravate neuronal tauopathy in bigenic mice. *Am J Pathol* 172: 786 – 798

Thomazeau A, Bosch M, Essayan-Perez S, Barnes SA, De Jesus-Cortes H, Bear MF (2020) Dissociation of functional and structural plasticity of dendritic spines during NMDAR and mGluR-dependent long-term synaptic depression in wild-type and fragile X model mice. *Mol Psychiatry* https://doi.org/10.1038/s41380-020-0821-6

Wagner FF, Benajiba L, Campbell AJ, Weïwer M, Sacher JR, Gale JP, Ross L, Puissant A, Alexe G, Conway A *et al* (2018) Exploiting an Asp-Glu "switch" in glycogen synthase kinase 3 to design paralog-selective inhibitors for use in acute myeloid leukemia. *Sci Transl Med* 10: eaam8460

Woodgett JR (1990) Molecular cloning and expression of glycogen synthase kinase-3/factor A. *EMBO J.* 9: 2431 – 2438

Yagishita S, Murayama M, Ebihara T, Maruyama K, Takashima A (2015) Glycogen synthase kinase 3β-mediated phosphorylation in the most C-terminal region of protein interacting with C kinase 1 (PICK1) regulates the binding of PICK1 to glutamate receptor subunit GluA2. *J Biol Chem* 290: 29438 – 29448

Yao HB, Shaw PC, Wong CC, Wan DCC (2002) Expression of glycogen synthase kinase-3 isoforms in mouse tissues and their transcription in the brain. *J Chem Neuroanat* 23: 291 – 297

Yuan Z, Agarwal-Mawal A, Paudel HK (2004) 14-3-3 binds to and mediates phosphorylation of microtubule-associated tau protein by Ser9-phosphorylated glycogen synthase kinase 3beta in the brain. *J Biol Chem* 279: 26105 – 26114

Zhou Q, Homma KJ, Poo MM (2004) Shrinkage of dendritic spines associated with long-term depression of hippocampal synapses. *Neuron* 44: 749 – 757

Zhu L-Q, Wang S-H, Liu D, Yin Y-Y, Tian Q, Wang X-C, Wang Q, Chen J-G, Wang J-Z (2007) Activation of glycogen synthase kinase-3 inhibits long-term potentiation with synapse-associated impairments. *J Neurosci* 27: 12211 – 12220